Polymer Chemistry

Cite this: *Polym. Chem.*, 2012, **3**, 1546

www.rsc.org/polymers

PAPER

Heteronucleobase-functionalized benzoxazine: synthesis, thermal properties, and self-assembled structure formed through multiple hydrogen bonding interactions

Wei-Hsun Hu, Kai-Wei Huang and Shiao-Wei Kuo*

Received 19th February 2012, Accepted 16th March 2012
DOI: 10.1039/c2py20090b

In this study we prepared a new class of thymine (T)-functionalized polybenzoxazine (PBZ) through the Michael addition of T to a new acryloyl-functionalized [(3-phenyl-3,4-dihydro-2*H*-benzooxazin-6-yl) methyl acrylate]benzoxazine (PA-ac) monomer and subsequent polymerization. We used ^{1}H and ^{13}C nuclear magnetic resonance spectroscopy and Fourier transform infrared (FTIR) spectroscopy to confirm the chemical structure of this new monomer and then employed differential scanning calorimetry (DSC) and FTIR spectroscopy to study the curing behavior of the new PBZ. The presence of the strongly self-complementary, multiply hydrogen-bonded T units in the PBZ matrix significantly enhanced its thermal stability, as evidenced from DSC traces and thermogravimetric analyses. Transition electron microscopy and wide-angle X-ray diffraction data provided evidence for the self-assembly of the PBZ occurring through self-complementary multiple hydrogen bonding of its T units.

Introduction

1,3-Benzoxazines are intriguing heterocyclic (oxazine-containing) compounds that have attracted considerable attention for their use as cyclic monomers. They are synthesized through the reactions of primary amines with phenol and formaldehyde; they can be polymerized through ring-opening polymerization in the absence of a catalyst, releasing no by-products.[1–3] Benzoxazine resins feature many attractive properties, including near-zero shrinkage upon polymerization, tunable glass transition temperatures, and high char yields.[4,5] Furthermore, polybenzoxazines (PBZs) have unique properties not found in traditional phenolic resins, such as excellent dimensional stability, flame retardance, stable dielectric constants, and low surface free energies.[6–10]

Procedures for the modification of benzoxazine resin are growing rapidly and many useful products are currently being developed.[11,12] To improve the performance of PBZs, polymerizable alkynyl and allyl side groups have been introduced into benzoxazine monomers.[13–20] These functionalized benzoxazines can be polymerized into products possessing three-dimensional networks that display high thermal and mechanical stability and high solvent and moisture resistances. Blending with other polymers,[21–24] including polyurethane, epoxy resin, and poly(*N*-vinyl-2-pyrrolidone), or organic–inorganic hybrid systems, including clay,[25–27] polyhedral oligomeric silsesquioxane (POSS),[28–35] and carbon nanotubes (CNTs),[36] also allows modification of the properties of benzoxazine resins.

The unusual properties of PBZs arise from the presence of extensively hydrogen-bonded networks.[11] Ishida *et al.* reported that the structures of PBZs are simply explained by the strength of their hydrogen bonding, which is dependent on the electronegativity of the side group attached to the nitrogen atom.[11] Recently, the use of strong, complementary, multiple hydrogen bonding has become very appealing for the development of macromolecules because such systems can potentially combine the advantages of synthetic functional polymers (low cost, high-yield preparation) with the supramolecular properties of, for example, DNA.[37] As a result, artificial PBZs bearing nucleobase moieties are very promising candidates for applications in supramolecular chemistry, molecular nanotechnology,[38–41] and biotechnology.[42–44] For example, Chang *et al.* successfully incorporated a supramolecular functionality, uracil, into a benzoxazine monomer through the reaction of a uracil-functionalized amine with phenol and formaldehyde.[45]

In this study, we synthesized a thymine (T)-functionalized benzoxazine monomer using a different synthetic route to avoid any possible side reactions of the uracil-functionalized amine during benzoxazine ring formation as shown in Scheme 1. First, we synthesized (3-phenyl-3,4-dihydro-2*H*-1,3-benzoxazin-6-yl) methanol (PA-OH) through the reaction of 4-hydroxybenzyl alcohol, aniline, and paraformaldehyde. Next, we prepared an acryloyl-functionalized benzoxazine (PA-ac) through the reaction of PA-OH with acryloyl chloride. Finally, we obtained the T-functionalized benzoxazine through the Michael addition of T to PA-ac. Because polymerization of this benzoxazine monomer

Department of Materials and Optoelectronic Science, Center for Nanoscience and Nanotechnology, National Sun Yat-Sen University, Kaohsiung, 804, Taiwan. E-mail: kuosw@faculty.nsysu.edu.tw

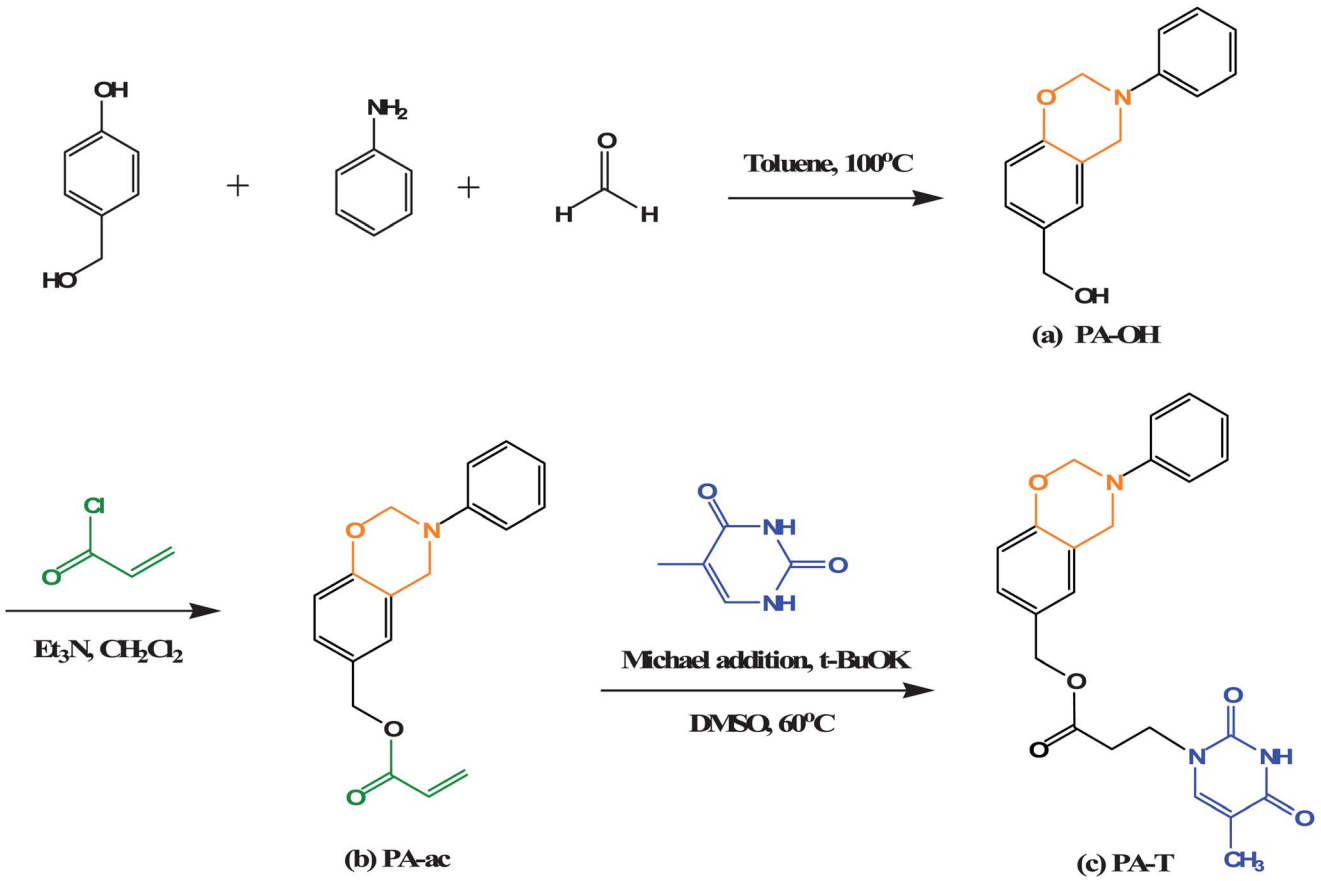

Scheme 1 Synthesis of (a) PA-OH, (b) PA-ac, and (c) PA-T.

results in a PBZ featuring a large number of strongly self-complementary, multiply hydrogen bonding T units, it exhibited notably improved thermal stability, as evidenced from differential scanning calorimetry (DSC) data and thermogravimetric analysis (TGA). In addition, we used transmission electron microscopy (TEM) and wide-angle X-ray diffraction (WAXD) analyses to characterize the self-assembled structure induced by self-complementary multiple hydrogen bonding interactions between the T groups.

Experimental

Materials

Paraformaldehyde (95%), aniline (99%), acryloyl chloride (97%), and 4-hydroxybenzyl alcohol (98%) were purchased from Aldrich. Thymine (99%) and KOBu were purchased from Showa. Toluene and dimethyl sulfoxide (DMSO) were distilled from CaH_2 under vacuum prior to use. All other chemicals were of reagent grade and used as received without further purification. The benzoxazine monomer 3-phenyl-2*H*,4*H*-benzooxazine (Pa) was prepared according to a previously reported procedure.[11]

(3-Phenyl-3,4-dihydro-2*H*-1,3-benzoxazin-6-yl)methanol (PA-OH).[46] 4-Hydroxybenzyl alcohol (4.96 g, 40.0 mmol) and paraformaldehyde (2.40 g, 80.0 mmol) were placed in a 100 mL three-necked flask cooled in an ice bath and then a solution of aniline (3.72 g, 40 mmol) in toluene (60 mL) was added. The mixture was then heated under reflux at 100 °C for 8 h. After cooling to room temperature, the solid residue was collected by filtration and recrystallized (toluene) to afford pale-yellow crystals (80%). ^{1}H NMR ($CDCl_3$, ppm): 4.55 (s, ArCH_2OH), 4.63 (s, CCH_2N), 5.36 (s, NCH_2O), 6.77–7.40 (m, Ar). ^{13}C NMR ($CDCl_3$, ppm): 50.48 (CCH_2N), 64.86 (ArCH_2OH), 79.45 (NCH_2O). IR (KBr, cm^{-1}): 3350 (OH stretching), 947 (out-of-plane CH bending).

(3-Phenyl-3,4-dihydro-2*H*-benzo[*e*][1,3]oxazin-6-yl)methyl acrylate (PA-ac).[47] Acryloyl chloride (2.71 g, 30.0 mmol) was added over 20 min to an ice-cooled solution of PA-OH (4.82 g, 20.0 mmol) and Et_3N (3.04 g, 30.0 mmol) in CH_2Cl_2 in a 100 mL flask. The solution was then stirred for 4 h at room temperature before being washed (1 M NaOH) and dried (Na_2SO_4). Evaporation of the solvent yielded yellowish crystals (90%). ^{1}H NMR ($CDCl_3$, ppm): 5.07 (s, CH_2OC=O), 4.63 (s, CCH_2N), 5.36 (NCH_2O), 6.15 (s, O=CCH=CH_2), 5.83 (s, CH=CH_2), 6.41 (s, CH=CH_2), 6.75–7.27 (m, Ar). ^{13}C NMR ($CDCl_3$, ppm): 50.48 (s, CCH_2N), 79.45 (s, NCH_2O), 66.13 (s, ArCH_2O), 129.25 (s, O=CH_2CH=CH_2), 131.10 (O=$CH_2$$C$H=$CH_2$), 165.45 (s, O=$CH_2$CH=$CH_2$). IR (KBr, cm^{-1}): 1730 (C=O), 1626 (C=C), 947 (out-of-plane CH bending).

(3-Phenyl-3,4-dihydro-2*H*-benzo[*e*][1,3]oxazin-6-yl)methyl thymine (PA-T). A solution of the benzoxazine PA-ac (0.51 g, 1.77 mmol)

in DMSO (60 mL) was added *via* syringe under N_2 to a mixture of T (2.23 g, 17.7 mmol) and KOBu^t (0.06 g, catalytic) in a round-bottom flask, which was then immersed in an oil bath and heated at 60 °C for 5 days. The resulting mixture was filtered to remove unreacted T and then the DMSO was evaporated under reduced pressure to yield a yellow product (85%). ^{1}H NMR (DMSO, ppm): 4.69 (s, CH_2OC=O), 4.63 (s, CCH_2N), 5.36 (s, NCH_2O), 2.61 (s, O=CCH_2CH$_2$N), 3.80 (s, O=CCH$_2$CH_2N), 7.53 (s, CH$_2$NCH=CCH$_3$), 1.74 (s, CH$_2$NCH=CCH_3), 11.30 (s, O=CNHC=O), 6.75–7.27 (m, Ar). ^{13}C NMR (DMSO, ppm): 50.48 (s, CCH$_2$N), 79.45 (s, NCH$_2$O), 66.13(s, ArCH$_2$O), 165.45 (s, O=CCH$_2$CH$_2$N), 33.03 (s, O=CCH$_2$CH$_2$N), 44.36 (s, O=CCH$_2$$CH_2$N), 142.25 (s, CH$_2NC$H=CCH$_3$), 108.41 (s, CH$_2$NCH=$CCH_3$), 11.95 (s, CH$_2$NCH=C$CH_3$), 151.2 (s, O=$C$NHC=O), 172.8 (s, O=CNH$C$=O). IR (KBr, cm^{-1}): 1677 (C=O), 3170 (NH), 945 (out-of-plane CH bending).

Pa and PA-T PBZs. Both the Pa and PA-T monomers are soluble in THF; their solutions were left to dry in air prior to curing. A desired amount of the benzoxazine monomer Pa or PA-T in THF solution was stirred for 2 h at room temperature and then poured onto an aluminium plate to dry for 6 h in the open air before being placed in an oven and heated at 100 °C under vacuum for 2 h. The cast film was then polymerized in a stepwise manner: at 140 and 160 °C for 3 h each and then at 200 °C for 4 h. Each cured sample was transparent and had a dark red color.

Characterization

^{1}H and ^{13}C nuclear magnetic resonance (NMR) spectra were recorded using an INOVA 500 instrument with $CDCl_3$ as the solvent and TMS as the external standard. Chemical shifts are reported in parts per million (ppm). FTIR spectra of the polymer blend films were recorded using the conventional KBr disk method. The films used in this study were sufficiently thin to obey the Beer–Lambert law. FTIR spectra were recorded using a Bruker Tensor 27 FTIR spectrophotometer; 32 scans were collected at a spectral resolution of 1 cm^{-1}. Because polymers containing OH groups are hygroscopic, pure N_2 gas was used to purge the spectrometer's optical box to maintain dry sample films. The dynamic curing kinetics were studied using a TA Q-20 differential scanning calorimeter operating under a N_2 atmosphere. The sample (*ca.* 7 mg) was placed in a sealed aluminium sample pan. Dynamic curing scans were conducted from 30 to 280 °C at a heating rate of 10 °C min^{-1}. The thermal stability of the samples was measured using a TA Q-50 thermogravimetric analyzer operated under a N_2 atmosphere. The cured sample (*ca.* 7 mg) was placed in a Pt cell and heated at a rate of 20 °C min^{-1} from 30 to 800 °C under a N_2 flow rate of 60 mL min^{-1}. Viscoelastic measurements of Pa and PA-T monomers were performed using an Anton Paar (Physica) MCR 301 rheometer operated in a parallel plate geometry; measurements were made at 80 °C. WAXD data were collected using the BL17A1 wiggler beamline of the National Synchrotron Radiation Research Center (NSRRC), Taiwan. A triangular bent Si (111) single crystal was employed to obtain a monochromated beam having a wavelength (λ) of 1.33001 Å. TEM images were recorded using a JEOL-2100 transmission electron microscope operated at an accelerating voltage of 200 kV. Ultrathin sections (thickness: *ca.* 70 nm) of the TEM samples were prepared using a Leica Ultracut UCT microtome equipped with a diamond knife. The ultrathin sections were placed onto Cu grids coated with carbon-supporting films and then stained through exposure to the vapor from 4% aqueous RuO_4 for 25 min.

Results and discussion

Synthesis of PA-T

Fig. 1 presents the ^{1}H NMR spectra of PA-OH, PA-ac, and PA-T. The spectrum of PA-OH [Fig. 1(a)] features two peaks at 4.63 and 5.36 ppm corresponding to the protons of the CH$_2$ bridge of the oxazine unit;[45] a singlet at 4.55 ppm represents the CH_2OH protons; the aromatic protons appeared as multiplets at 6.77–7.40 ppm. In Fig. 1(b), the singlet at 5.07 ppm for the CH_2OC=O protons of PA-ac is shifted significantly from the signal for the CH_2OH protons of PA-OH [4.55 ppm in Fig. 1(a)]; the vinyl group is represented by signals at 5.83, 6.15, and 6.41 ppm (relative ratio: 1 : 1 : 1) corresponding to the *cis*, *trans*, and substituted vinyl protons, respectively.[51] The signals for these vinyl protons peaks disappeared after Michael addition of T, confirming the complete consumption of PA-T [Fig. 1(c)].[48] The signals from the T unit's CH$_3$ (H_g), O=CCH_2CH$_2$N (H_d), and O=CCH_2CH$_2$N (H_e) protons appear at a relative ratio of 3 : 2 : 2 at 1.74, 2.61 and 3.80 ppm, respectively; the NH unit of the T group appears as a signal at 11.30 ppm. Most importantly, the peaks at 4.63 and 5.36 ppm, corresponding to the CH$_2$ bridge of the oxazine unit, remained for the T-functionalized monomer. Fig. 1 provides assignments of all of the other peaks.

Fig. 2 presents the ^{13}C NMR spectra of PA-OH, PA-ac, and PA-T. In Fig. 2(a), two peaks appear at 50.48 and 79.45 ppm in the spectrum of PA-OH, corresponding to characteristic resonances of the carbon nuclei of the oxazine ring; the resonance at 64.86 ppm for the ArCH$_2$OH nucleus of PA-OH is shifted slightly downfield to 66.13 ppm in the spectrum of PA-ac [Fig. 2(b)], which features signals at 129.25, 131.10, and 165.45 ppm for the C=CC=O, C=CC=O, and C=CC=O units, respectively. The signals for these vinyl carbon nuclei

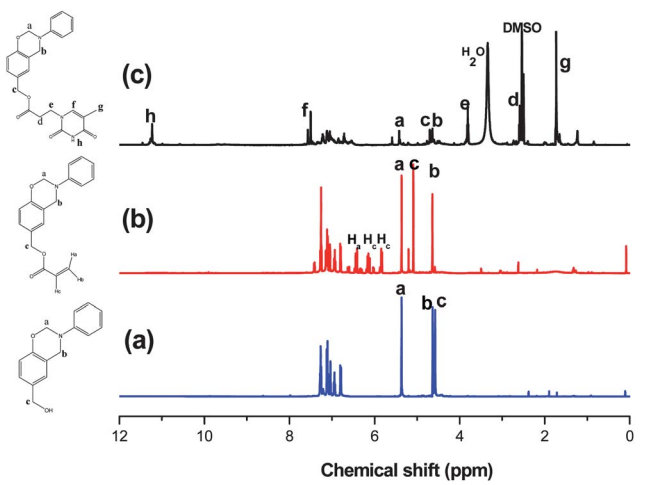

Fig. 1 ^{1}H NMR spectra of (a) PA-OH and (b) PA-ac in $CDCl_3$ and (c) PA-T in d_6-DMSO.

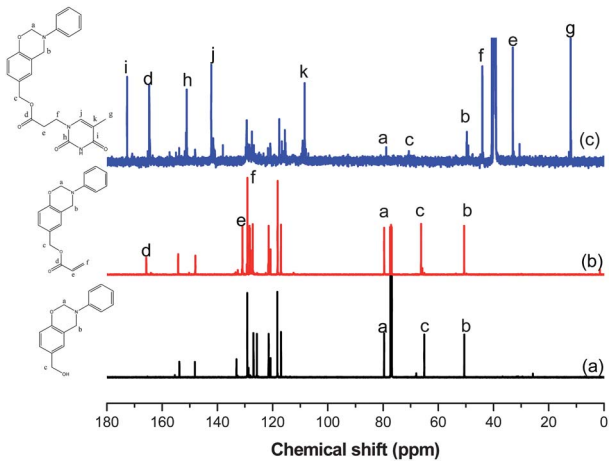

Fig. 2 ^{13}C NMR spectra of (a) PA-OH and (b) PA-ac in $CDCl_3$ and (c) PA-T in d_6-DMSO.

disappeared after Michael addition of T, again confirming the complete consumption of PA-T [Fig. 2(c)]. The signal for the C═O group of PA-ac at 165.45 ppm [Fig. 2(b)] did not change after Michael addition, but signals for two new C═O groups from T (N*CO*NH, NH*CO*CCH$_3$) appeared at 151.2 and 172.8 ppm [Fig. 2(c)], also indicating the successful synthesis of PA-T. The signals at 50.48 and 79.45 ppm, corresponding to the CH_2 bridge nuclei of the oxazine unit, did not disappear after acryloyl- and T-functionalization. Fig. 2 provides assignments for all of the other peaks. Fig. 3 presents FTIR spectra of PA-OH, PA-ac, and PA-T recorded at room temperature.

The spectrum of PA-OH reveals [Fig. 3(a)] a broad signal for the OH group at 3350 cm^{-1}; signals for the C–C stretching vibrations of the 1,2,4-substituted benzene ring at 1499 and 947 cm^{-1}; and a signal for the asymmetric C–O–C stretching at 1236 cm^{-1}. In the spectrum of PA-ac [Fig. 3(b)], a signal for the OH group is almost absent, but a new signal for a C═O group appears at 1730 cm^{-1}. In Fig. 3(c), absorptions of the amide I and secondary amino groups of PA-T appear as signals at 1677 and 3170 cm^{-1}, respectively, confirming that the C═O and

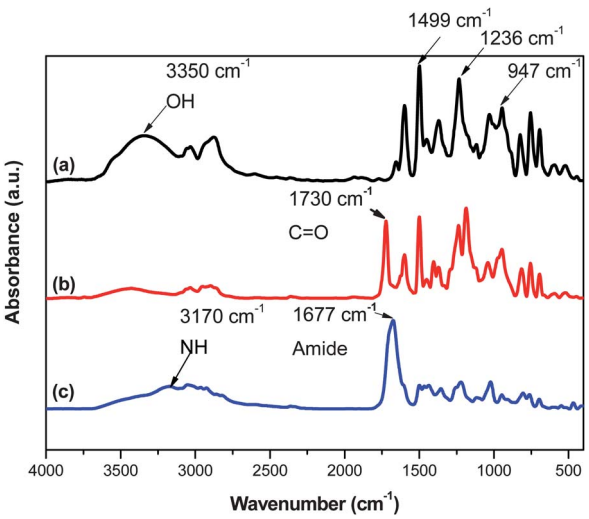

Fig. 3 FTIR spectra of (a) PA-OH and (b) PA-ac and (c) PA-T.

T functionalities had participated in the Michael addition. The signals of the benzoxazine ring at 1499 and 947 cm^{-1} remained present after acryloyl- and T-functionalization. Together, all of the ^1H NMR, ^{13}C NMR, and FTIR spectroscopic data confirmed the successful synthesis of PA-T.

Thermal polymerization and stability of PA-T

We used DSC analysis to investigate the curing behavior of pure PA-OH, PA-ac, and PA-T. The DSC trace of the uncured PA-OH [Fig. 4(a)] featured an exotherm with a maximum at 245.0 °C, with a heat of polymerization of 233.4 J g^{-1}. Fig. 4(b) presents the DSC profile of PA-ac, featuring an exotherm peak at 217.4 °C (a lower temperature than that of PA-OH), with a total heat of polymerization of 325.3 J g^{-1} (higher than that of PA-OH). It appears that the presence of vinyl functional groups of PA-ac assisted the ring opening of the oxazine ring during the curing process.[11] In addition, the vinyl group of PA-ac behaved as an additional curing site, resulting in the total heat from the exotherm peak being higher than that from PA-OH. The exotherm peak for the monomer PA-T appeared at 205.8 °C, a lower temperature than that of either PA-OH or PA-ac. Ronda *et al.* reported that the incorporation of electron donating or withdrawing groups onto the benzoxazine structure will change the properties of the exothermic peak.[49] The strong, multiple hydrogen bonding interactions of the T group in the monomer PA-T also led to the dramatic decrease in the polymerization temperature. The T group catalyzed the polymerization by increasing the concentration of oxonium species in the medium. Furthermore, the strongly activating T group increased the number of propagation pathways, due to the presence of multiple nucleophilic *ortho* positions. The total exotherm for the monomer PA-T was 41.1 J g^{-1}, lower than those of PA-OH and PA-ac, as would be expected. Fig. 5 displays DSC curves of pure PA-T recorded after thermal curing at different temperatures. The size of the exotherm peak decreased upon increasing the curing temperature, disappearing almost completely after curing at 180 °C. To determine which reaction was involved in the exotherm of the DSC traces, we used FTIR spectroscopy to characterize the curing process of the pure PA-T at different

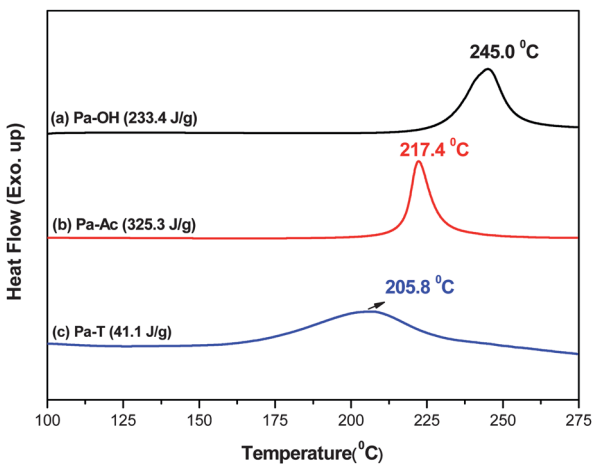

Fig. 4 DSC thermograms of uncured (a) PA-OH, (b) PA-ac, and (c) PA-T.

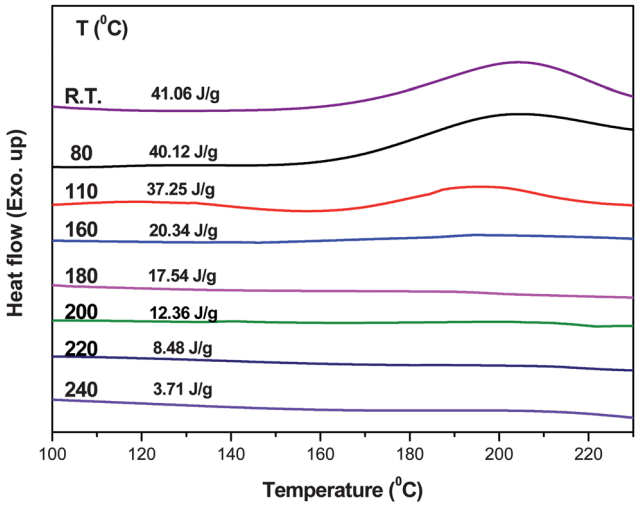

Fig. 5 DSC thermograms of the PA-T benzoxazine monomer recorded after each heating stage.

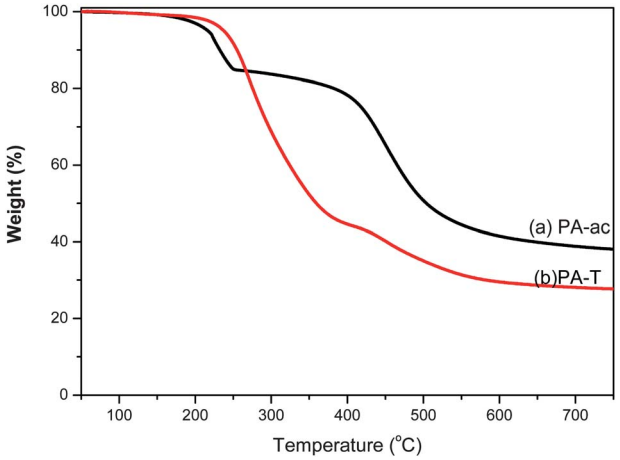

Fig. 7 TGA thermograms of uncured (a) PA-ac and (b) PA-T.

temperatures. In Fig. 6(a), we assign the bands at 1498 and 943 cm^{-1} to the trisubstituted aromatic ring in the benzoxazine structure of PA-T.[11] The broad absorption band at 2500–3500 cm^{-1} in Fig. 6(b)–(g) represents the different types of hydrogen bonding interactions, including intramolecular O–H···N, intermolecular O–H···O, and self-association T···T hydrogen bonding. In addition, the signals of the free and hydrogen-bonded C=O groups of the T units appeared at 1700 and near 1680 cm^{-1}, respectively.[50] The wavenumber and intensity of the signal for the free C=O groups of PA-T changed upon increasing the temperature, consistent with the heat disrupting the hydrogen bonding interactions.

Fig. 7 displays the TGA traces of PA-ac and PA-T, recorded under N_2. For PA-ac, a sharp decomposition appeared at 195 °C, representing a weight loss of 12 wt%. This result is similar to that reported by Ishida, who found that the $CH_2CC{=}O$ linkage in the monomer was a weak structure that broke upon heating.[47] The thermal stability of PA-T was better than that of PA-ac because of the strong self-association of the T units. The char yield of PA-T was, however, lower than that of PA-ac because the vinyl groups of the latter resulted in increased cross-linking.

Thermal polymerization and properties of the Pa and PA-T PBZs

Based on rheological analyses, the viscosity of the monomer PA-T (*ca.* 460 Pa s at 80 °C) was significantly greater than that of the monomer Pa (*ca.* 1.1 Pa s at 80 °C), due to the strong complementary multiple hydrogen bonding of the T units. Fig. 8 displays the curing exotherms of neat Pa and of binary mixtures of Pa and PA-T at various weight ratios. The curing exotherm of the synthesized Pa revealed an onset temperature of 200 °C with a peak temperature of 245 °C. The curing peak shifted to lower temperature upon increasing the PA-T content in the binary mixture; for example, it shifted to 195 °C for the Pa/PA-T = 60/40 system. Such accelerated curing suggests that PA-T acted as a catalyst for the polymerization of the Pa benzoxazine resin.[11] The curing peaks in the exotherms of the binary mixtures broadened upon increasing the PA-T content;

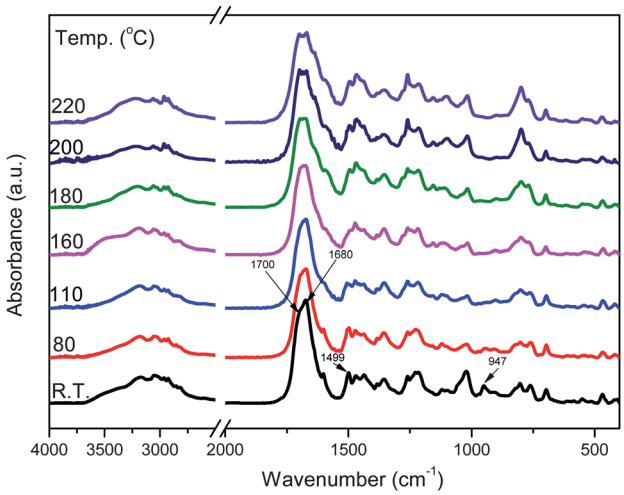

Fig. 6 FTIR spectra of the PA-T benzoxazine monomer recorded after each heating stage.

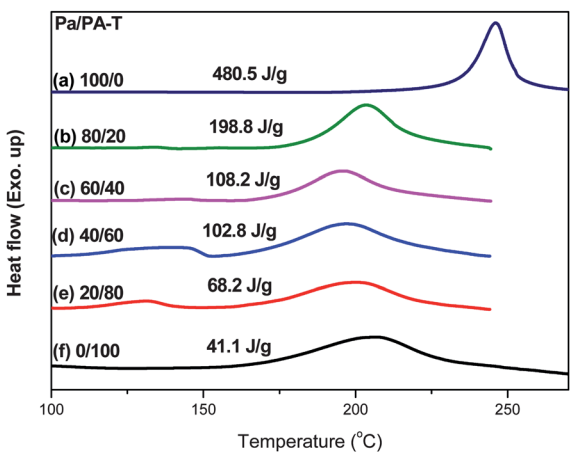

Fig. 8 Curing behavior, determined through DSC analyses, of Pa/PA-T mixtures at various PA-T contents.

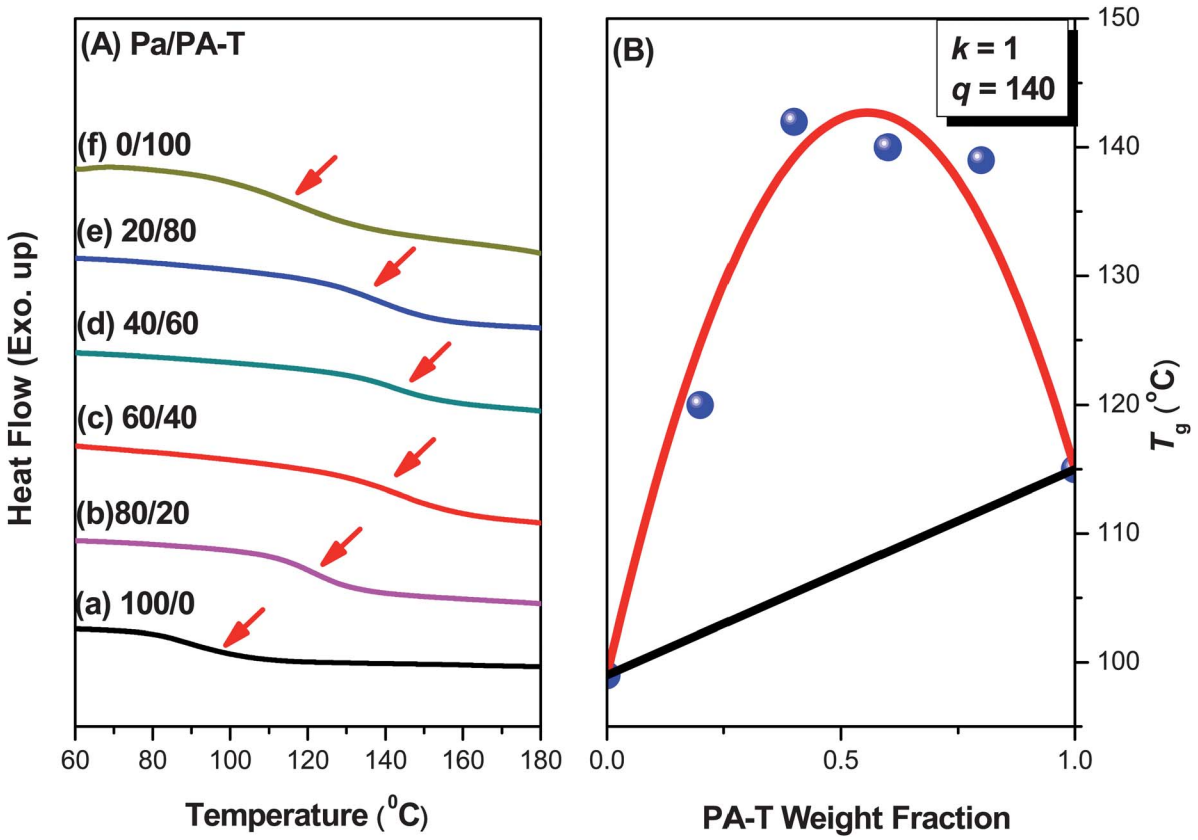

Fig. 9 (A) DSC analyses of Pa/PA-T benzoxazine copolymers at various PA-T contents after curing. (B) Glass transition temperatures of the Pa/PA-T benzoxazine copolymers, determined using the Kwei equation.

furthermore, the area under the exothermal peaks decreased, from 480.5 J g^{-1} for pure Pa to 41.06 J g^{-1} for pure PA-T, as would be expected.

We used DSC to examine the glass transition behavior of the Pa and PA-T copolymers [Fig. 9(A)]. For pure Pa and pure PA-T, the glass transition temperatures (T_g's) were 100 and

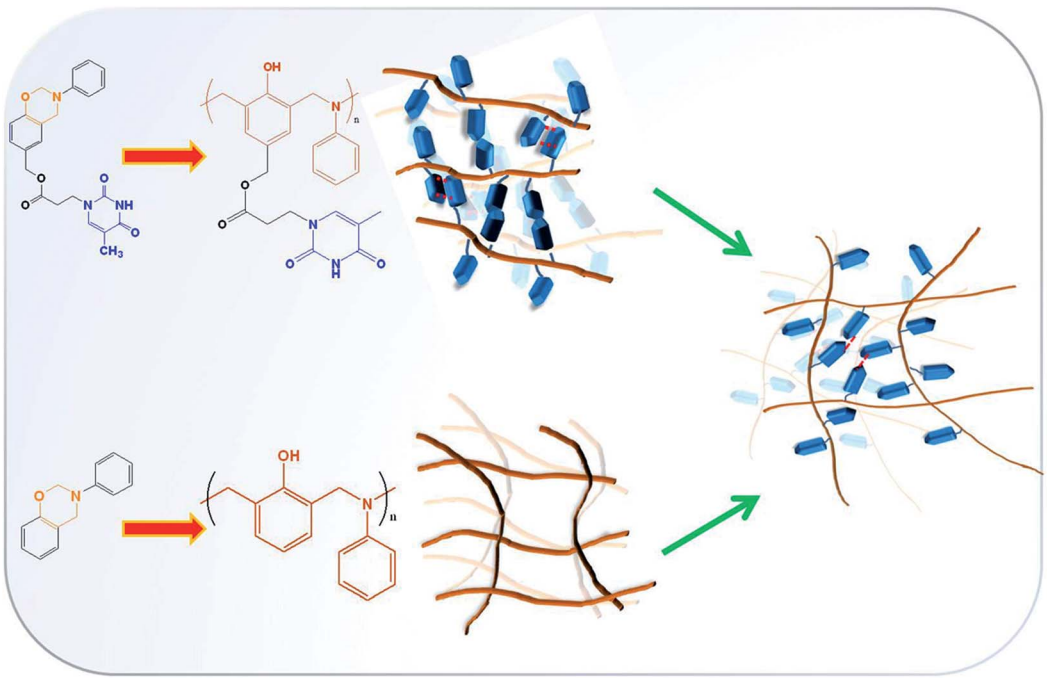

Scheme 2 Chemical structures and morphologies of PA-T, Pa, and their corresponding Pa/PA-T PBZs.

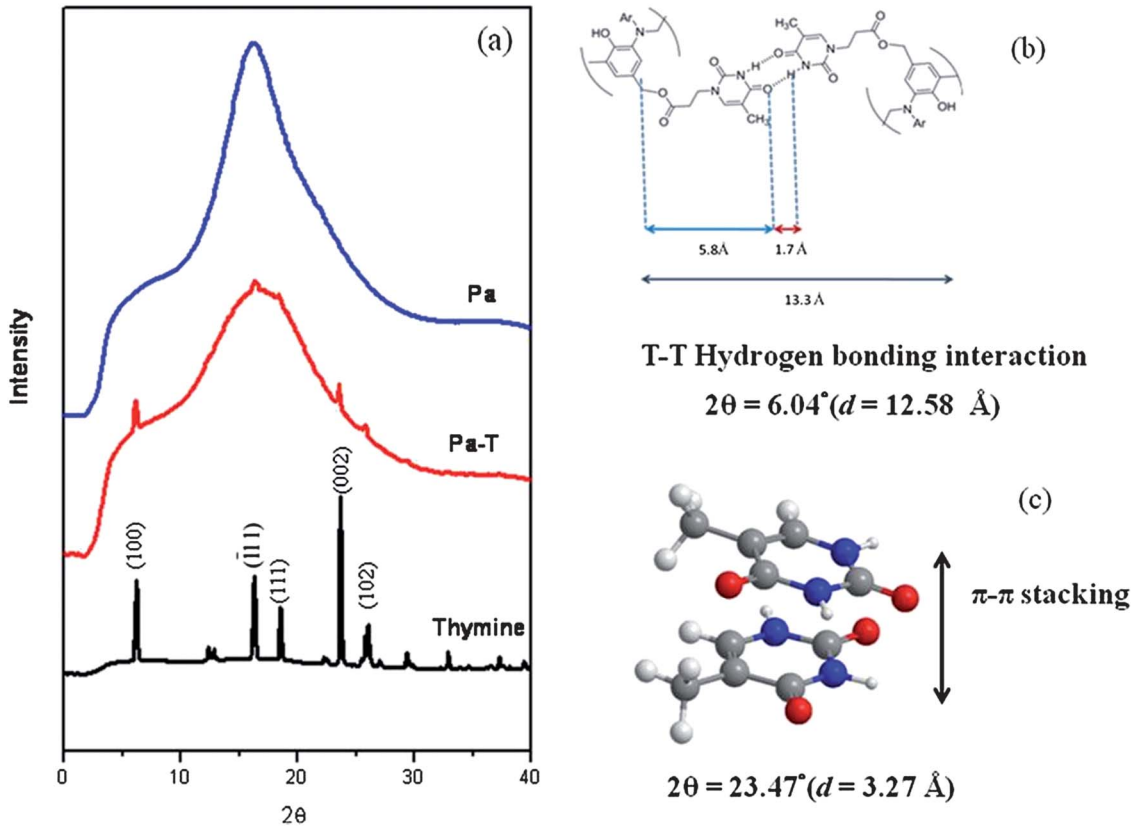

Fig. 10 (a) WAXD patterns of Pa, PA-T, and T. (b and c) Schematic representations of (b) multiple hydrogen bonding and (c) π–π stacking interactions of the T units in PA-T PBZ.

115 °C, respectively. In addition, the DSC thermograms of the Pa/PA-T benzoxazine copolymers at various compositions revealed only a single glass transition. A single value of T_g strongly suggests that the polymers were fully miscible with a homogeneous amorphous phase. Meanwhile, the values of T_g for the copolymers were higher than that of either individual PBZ. The Kwei equation[51] is usually employed to characterize systems displaying specific interactions:

$$T_g = \frac{W_1 T_{g1} + k W_2 T_{g2}}{W_1 + k W_2} + q W_1 W_2 \quad (1)$$

where W_1 and W_2 are the weight fractions of the components, T_{g1} and T_{g2} are the corresponding glass transition temperatures, and k and q are fitting constants. The parameter q represents the strength of the specific interactions in the system; it reflects a balance between the breaking of self-association interactions and the forming of inter-association interactions. From nonlinear least-squares "best fits" of the plots [Fig. 9(B)] for the Pa/PA-T benzoxazine copolymers, we obtained values of k and q of 1 and 140, respectively. A positive value of q usually suggests that strong specific intermolecular interactions exist between the two polymers.[24,52,53] We suggest that our positive value of q arose from two factors. In general, a PBZ possesses a high crosslinking density even without the addition of catalysts or initiators. Sawaryn *et al.* reported, however, that blocking of the *para* position of the phenolic ring can prevent network formation, resulting in the PBZ tending to form linear chains.[54] As a result, we would expect pure Pa to form a network of crosslinks in its polymerized structure, but without strong, self-complementary, multiple hydrogen bonding interactions; therefore, its value of T_g was approximately 100 °C. In contrast, pure PA-T features the strong, self-complementary, multiple hydrogen bonding of its T units, but it lacks the network of chemical crosslinks in its polymerized structure, due to substitution at the *para* position of the phenolic ring; therefore, its value of T_g was slightly higher, at approximately 115 °C. The advantages of both a network of chemical crosslinks and strong, self-complementary, multiple hydrogen bonding of T units like physical crosslinks occurred, however, in the Pa/PA-T benzoxazine copolymers, as indicated in Scheme 2. Therefore, the values of T_g of the Pa/PA-T benzoxazine copolymers were higher than that of either individual PBZ.

Self-assembled structures induced by multiple hydrogen bonding interactions

DNA and RNA are unique biomolecules that allow the formation of a variety of self-assembled nanostructures.[55–58] Therefore,

Table 1 Diffraction peaks, *d*-spacing, and Miller index of PA-T PBZ

2θ	*d*-spacing (Å)	*hkl*
6.06	12.58	100
16.26	4.70	ī11
18.67	4.09	111
23.47	3.27	002
25.94	2.96	102

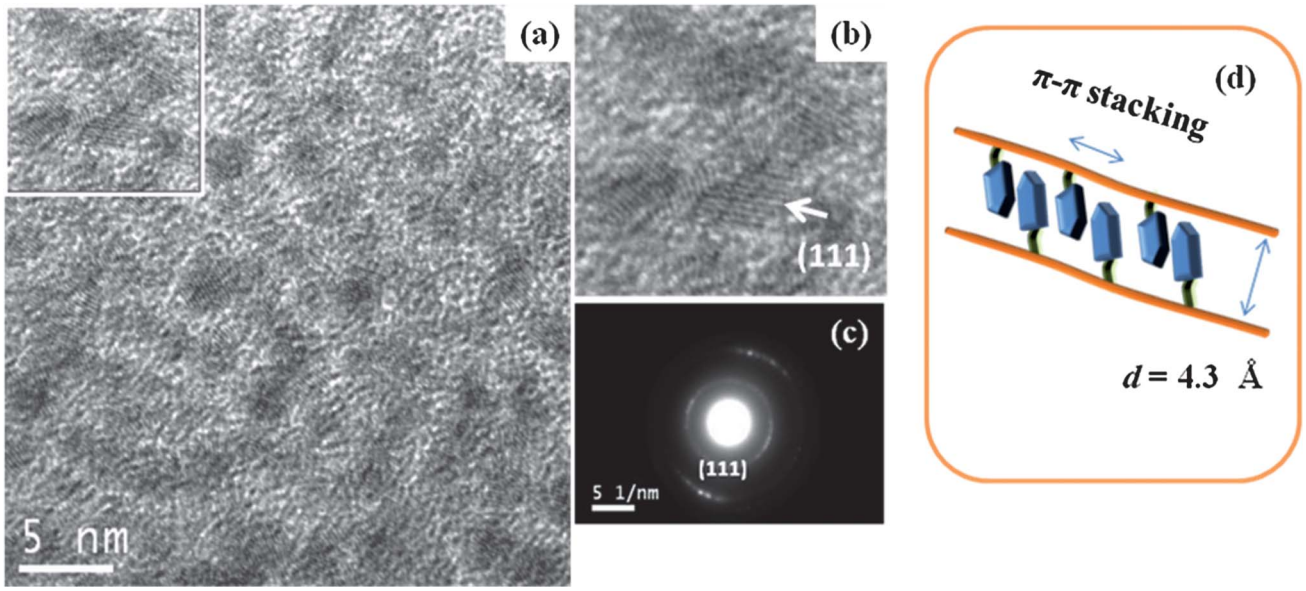

Fig. 11 (a and b) High-resolution TEM images and (c) SAED pattern of PA-T PBZ. (d) Schematic representation of the images in (a) and (b), displaying the packing of the T units on the side chains through π–π stacking.

we were interested in investigating the self-assembly of our PBZs. The WAXD pattern of Pa revealed an amorphous structure [Fig. 10(a)], but that of PA-T displayed some crystal diffraction peaks, the positions and relative intensities of which matched well with those of the standard low-molecular-weight compound T. Table 1 summarizes the relationship between the values of 2θ, the *d*-spacings, and the Miller index, which were all consistent with the XRD data for T itself (JPPDS no. 39-1576). The peak at a value of 2θ of 6.04° provides a value of *d* of 12.58 Å, which is close to the distance between the side chains of the PA-T PBZ, as displayed in the calculated structure (Spartan software) in Fig. 10(b). The self-complementary multiple hydrogen bonds between the T units led to greater packing of the PBZ and expanded the inter-chain spacing.[59] In addition, the signal at a value of 2θ of 23.47° provided a value of *d* of 3.27 Å that is consistent with the π–π stacking of T units in the inter-layer [Fig. 11(c)].[60,61] Fig. 11 displays high-resolution TEM images of the microstructure of the pure PA-T PBZ. We can find the self-assembly alternating packing in the TEM image; the long period of packing is approximately 4–4.5 Å. After RuO_4 staining, we attribute the dark regions to benzene rings, leading to high mass contrast. Furthermore, we used selected-area electron diffraction (SAED) to determine the crystal structure of the PA-T PBZ. The diffraction pattern in Fig. 11(c) is close to an arc-ring, due to the semi-ordered packing in the PBZ induced by T···T interactions. The *d*-spacing of the first arc-ring, calculated from the reciprocal lattice, was 4.3 Å, consistent with our results from the WAXD pattern. The orientation of the packing (111) is consistent with the presence of T units interacting on the side chains of the PBZ through π–π stacking between T layers [Fig. 11(d)].[62,63] Moreover, the TEM image also suggests that the structure of the PBZ tended toward linearity. The T units served as blocking groups that prohibited *para* substitution of the phenolic ring; as a result, network formation was prevented and we obtained a linear PBZ.[54] Because of the T units in the PBZ matrix, it is easy to form multiple hydrogen bonds with adenine (A) or diaminopyridine units and form a supramolecular structure through simple blending.

Conclusions

We have synthesized a novel T-functionalized benzoxazine (PA-T) by the Michael addition of T to PA-ac. TGA revealed that the presence of the T units increased the decomposition temperature of PA-T relative to that of PA-ac. In addition, the strong multiple hydrogen bonds of the T units in PA-T led to a dramatic decrease in its polymerization temperature. The T units appeared to catalyze the polymerization by increasing the concentration of oxonium species in the medium. Taking advantage of both the network of crosslinked structures and the strong self-complementary multiple hydrogen bonds of the T unit groups, the Pa/PA-T benzoxazine copolymers exhibited higher values of T_g than that of either individual PBZ. In addition, TEM images and diffraction patterns revealed a linear-like structure for the PA-T PBZ, with self-assembly through packing of its T units.

Acknowledgements

This study was supported financially by the National Science Council, Taiwan, Republic of China, under contracts NSC 100-2221-E-110-029-MY3 and NSC 100-2628-E-110-001.

References

1 C. P. R. Nair, *Prog. Polym. Sci.*, 2004, **29**, 401.
2 H. Xiang and Y. Gu, *Mater. Rev.*, 2004, **18**, 51.
3 N. N. Ghosh, B. Kiskan and Y. Yagci, *Prog. Polym. Sci.*, 2007, **32**, 1344.
4 T. Takeichi, T. Kawauchi and T. Agag, *Polym. J.*, 2008, **40**, 1121.
5 H. Ishida and D. J. Allen, *J. Polym. Sci., Part B: Polym. Phys.*, 1996, **34**, 1019.

6 Y. Yagci, B. Kiskan and N. N. Ghosh, *J. Polym. Sci., Part A: Polym. Chem.*, 2009, **47**, 5565.
7 C. F. Wang, Y. C. Su, S. W. Kuo, C. F. Huang, Y. C. Sheen and F. C. Chang, *Angew. Chem., Int. Ed.*, 2006, **45**, 2248.
8 S. W. Kuo, Y. C. Wu, C. F. Wang and K. U. Jeong, *J. Phys. Chem. C*, 2009, **113**, 20666.
9 C. F. Wang, S. F. Chiou, F. H. Ko, J. K. Chen, C. T. Chou, C. F. Huang, S. W. Kuo and F. C. Chang, *Langmuir*, 2007, **23**, 5868.
10 C. F. Wang, F. C. Chang and S. W. Kuo, in *Handbook of Polybenzoxazine*, ed. H. Ishida and T. Agag, Elsevier, Amsterdam, 2011, ch. 33, p. 579.
11 H. Ishida, in *Handbook of Polybenzoxazine*, ed. H. Ishida and T. Agag, Elsevier, Amsterdam, 2011, ch. 1, p. 1.
12 X. Li and Y. Gu, *Polym. Chem.*, 2011, **2**, 2778.
13 A. Chernykh, T. Agag and H. Ishida, *Polymer*, 2009, **50**, 3153.
14 T. Agag and T. Takeichi, *Macromolecules*, 2001, **34**, 7257.
15 T. Agag and T. Takeichi, *Macromolecules*, 2003, **36**, 6010.
16 K. S. Kumar, C. P. Nair, T. S. Radhakrishnan and K. N. Ninan, *Eur. Polym. J.*, 2007, **43**, 2504.
17 B. Kiskan and Y. Yagci, *Polymer*, 2004, **49**, 2455.
18 B. Kiskan, B. Aydoan and Y. Yagci, *J. Polym. Sci., Part A: Polym. Chem.*, 2009, **47**, 804.
19 A. Chernykh, T. Agag and H. Ishida, *Macromolecules*, 2009, **42**, 5121.
20 S. W. Kuo and W. C. Liu, *J. Appl. Polym. Sci.*, 2010, **117**, 3121.
21 H. Ishida and Y. H. Lee, *Polymer*, 2001, **42**, 6971.
22 T. Takeichi, T. Agag and R. Zeidam, *J. Polym. Sci., Part A: Polym. Chem.*, 2001, **39**, 2633.
23 T. Takeichi and Y. Guo, *Polym. J.*, 2001, **33**, 437.
24 Y. C. Su, S. W. Kuo, H. Y. Xu and F. C. Chang, *Polymer*, 2003, **44**, 2187.
25 T. Agag and T. Takeichi, *Polymer*, 2000, **41**, 7083.
26 P. Phirivawirut, R. Magaraphan and H. Ishida, *Mater. Res. Innovations*, 2001, **4**, 187.
27 H. K. Fu, C. F. Huang, S. W. Kuo, H. C. Lin, D. R. Yei and F. C. Chang, *Macromol. Rapid Commun.*, 2008, **29**, 1216.
28 J. Zhang, R. Xu and D. Yu, *Eur. Polym. J.*, 2007, **43**, 743.
29 Q. Chen, R. Xu, J. Zhang and D. Yu, *Macromol. Rapid Commun.*, 2005, **26**, 1878.
30 Y. Liu and S. Zheng, *J. Polym. Sci., Part A: Polym. Chem.*, 2006, **44**, 1168.
31 J. M. Huang, S. W. Kuo, H. J. Huang, Y. X. Wang and Y. T. Chen, *J. Appl. Polym. Sci.*, 2009, **111**, 628.
32 Y. C. Wu and S. W. Kuo, *Polymer*, 2010, **51**, 3948.
33 K. W. Huang and S. W. Kuo, *Macromol. Chem. Phys.*, 2010, **211**, 2301.
34 K. W. Huang and S. W. Kuo, *Polym. Compos.*, 2011, **32**, 1086.
35 S. W. Kuo and F. C. Chang, *Prog. Polym. Sci.*, 2011, **36**, 1649.
36 R. Xu, P. Zhang, J. Wang and D. Yu, in *Handbook of Polybenzoxazine*, ed. H. Ishida and T. Agag, Elsevier, Amsterdam, 2011, ch. 31, p. 541.
37 S. Sivakova and S. J. Rowan, *Chem. Soc. Rev.*, 2005, **34**, 9.
38 A. K. Boal, F. Ilhan, J. E. DeRouchey, T. Thurn-Albrecht, T. P. Russell and V. M. Rotello, *Nature*, 2000, **404**, 746.
39 F. Ilhan, T. H. Galow, M. Gray, G. Clavier and V. M. Rotello, *J. Am. Chem. Soc.*, 2000, **122**, 5895.
40 R. J. Thibault, P. J. Hotchkiss, M. Gray and V. M. Rotello, *J. Am. Chem. Soc.*, 2003, **125**, 11249.
41 O. Uzun, A. Sanyal, H. Nakade, R. J. Thibault and V. M. Rotello, *J. Am. Chem. Soc.*, 2004, **126**, 14773.
42 J. E. Puskas, Y. Dahman, A. Margaritis and M. Cunningham, *Biomacromolecules*, 2004, **5**, 1412.
43 A. Marsh, A. Khan, M. Garcia and D. M. Haddleton, *Chem. Commun.*, 2000, 2083.
44 P. Wittung, P. E. Nielsen, O. Buchardt, M. Egholm and B. Norden, *Nature*, 1994, **368**, 561.
45 Y. C. Yen, C. C. Cheng, Y. L. Chu and F. C. Chang, *Polym. Chem.*, 2011, **2**, 1648.
46 Y. C. Su, W. C. Chen, K. L. Ou and F. C. Chang, *Polymer*, 2005, **46**, 3758.
47 L. Jin, T. Agag, Y. Yagci and H. Ishida, *Macromolecules*, 2011, **44**, 767.
48 A. S. Karikari, B. D. Mather and T. E. Long, *Biomacromolecules*, 2007, **8**, 302.
49 R. Andreu, J. A. Reina and J. C. Ronda, *J. Polym. Sci., Part A: Polym. Chem.*, 2008, **46**, 3353.
50 S. W. Kuo and S. T. Tsai, *Macromolecules*, 2009, **42**, 4701.
51 T. Kwei, *J. Polym. Sci., Polym. Lett. Ed.*, 1984, **22**, 307.
52 W. C. Chen, S. W. Kuo, U. S. Jeng and F. C. Chang, *Macromolecules*, 2008, **41**, 1401.
53 S. C. Chen, S. W. Kuo, C. S. Liao and F. C. Chang, *Macromolecules*, 2008, **41**, 8865.
54 C. Sawaryn, K. Landfester and A. Taden, *Macromolecules*, 2011, **44**, 7668.
55 W. Mamdouh, R. E. A. Kelly, M. Dong, L. N. Kantorovich and F. Besenbacher, *J. Am. Chem. Soc.*, 2008, **130**, 695.
56 J. Cortese, C. Soulié-Ziakovic, M. Cloitre, S. Tencé-Girault and L. Leibler, *J. Am. Chem. Soc.*, 2011, **133**, 19672.
57 J. Jung, J. C. Kim, Y. Rho, M. Kim, W. Kwon, H. Kim and M. Ree, *ACS Appl. Mater. Interfaces*, 2011, **3**, 2655.
58 J. S. Park, G. S. Lee, Y. J. Lee, Y. S. Park and K. B. Yoon, *J. Am. Chem. Soc.*, 2002, **124**, 13366.
59 J. Zhang, R. Xu and D. Yu, *Eur. Polym. J.*, 2007, **43**, 743.
60 C. C. Cheng, Y. C. Yen, Y. S. Ye and F. C. Chang, *J. Polym. Sci., Part A: Polym. Chem.*, 2008, **46**, 3353.
61 S. Sivakova, D. A. Bohnsack, M. E. Mackay, P. Suwanmala and S. J. Rowan, *J. Am. Chem. Soc.*, 2005, **127**, 18202.
62 W. Xu, R. E. A. Kelly, R. Otero, M. Schöck, E. Lægsgaard, I. Stensgaard, L. N. Kantorovich and F. Besenbacher, *Small*, 2007, **3**, 2011.
63 T. R. Lu, L. C. Chen, K. H. Chen, D. M. Bhusari, T. M. Chen and C. T. Kuo, *Thin Solid Films*, 1998, **322**, 74.

